Long-range ordering and local structural disordering of $BiAgSe_2$ and BiAgSeTe thermoelectric

Weifeng Huang [a], Yingcai Zhu[b], Yong Liu[c*], Shi Tao [d], Changchun Yang [a], Qianshun Diao[b], Zhen Hong[b], Haijiao Han[b], Lijuan Liu [e], Wei Xu [b*]

[a] School of Electronic Engineering, Jiujiang University, Jiujiang, 332005, China

[b] Beijing Synchrotron Radiation Facility, Institute of High Energy Physics Chinese Academy of Sciences, Beijing, 100049, China.

[c] Foshan (Southern China) Institute for New Materials, Foshan, 528200, Guangdong, P. R. China

[d]School of Electronic and Information Engineering, Jiangsu Laboratory of Advanced Functional Materials, Changshu Institute of Technology, Changshu 215500, China

[e] School of Physics and Microelectronics, Zhengzhou University, Zhengzhou, Henan 450001, China

Table.S1 Crystallographic information of $BiAgSe_2$, $BiAgTe_2$, Bi_2Se_3

$BiAgSe_2$-α-phase	$Pm\bar{3}1$, **SG. No.164,a=b=4.18 Å , c= 19.67Å** **α=β=90°， γ=120°**				
	x	y	z	Occupation	Wyckoff site
Ag	0	0	0	1	1a
Bi	0	0	0.5	1	1b
Ag	0.333333	0.666667	0.672	1	2d
Bi	0.333333	0.666667	0.163	1	2d
Se	0	0	0.253	1	2c
Se	0.333333	0.666667	0.926	1	2d
Se	0.333333	0.666667	0.406	1	2d
$BiAgSe_2$-β-phase	$R\bar{3}m$, **SG No.166, a=b= 4.201Å, c=18.865 Å** **α=β=90°, γ=120°**				
	x	y	z	Occupation	Wyckoff site
Ag	0	0	0	1	3a
Bi	0	0	0.5	1	3b
Se	0	0	0.254	1	6c
$BiAgSe_2$-γ-phase	$Fm\bar{3}m$， **SG No.225, a=b= 5.832Å** **α=β=90°, γ=120°**				
	x	y	z	Occupation	Wyckoff site
Ag	0	0	0	0.5	4a
Se	0.5	0.5	0.5	1	4b
Bi	0	0	0	0.5	4a
$BiAgTe_2$	$R\bar{3}m$, **SG No.166, a=b= 4.453Å, c=20.954 Å** **α=β=90°, γ=120°**				
	x	y	z	Occupation	Wyckoff site
Ag	0	0	0	1	3a
Bi	0	0	0.5	1	3b
Te	0	0	0.744	1	6c

*Correspondence should be addressed to xuw@mail.ihep.ac.cn and liuy08@qq.com

Bi_2Se_3	$R\bar{3}m$, SG No.166, a=b= 4.191Å, c=29.929Å α=β=90°, γ=120°				
	x	y	z	Occupation	Wyckoff site
Bi	0	0	0.398	1	6c
Se	0	0	0.216	1	6c
Se	0	0	0	1	3a

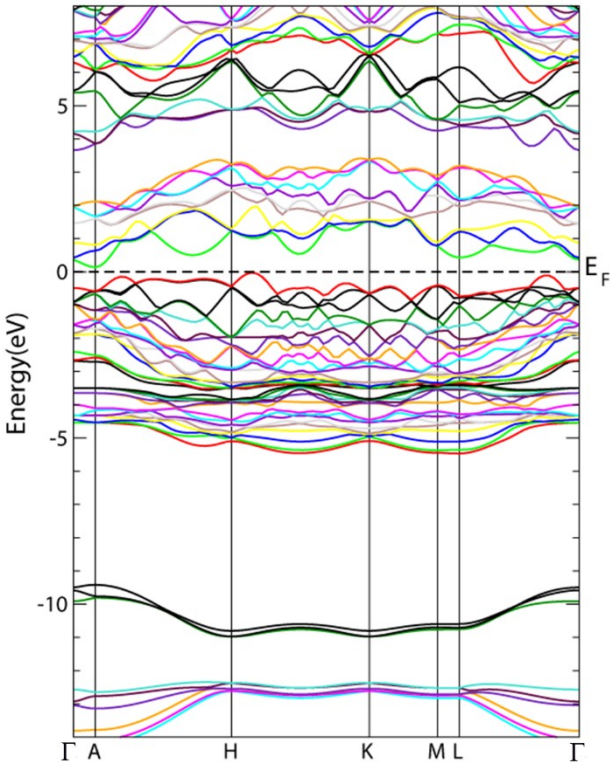

Figure.S1 Electronic band structure of α-$BiAgSe_2$

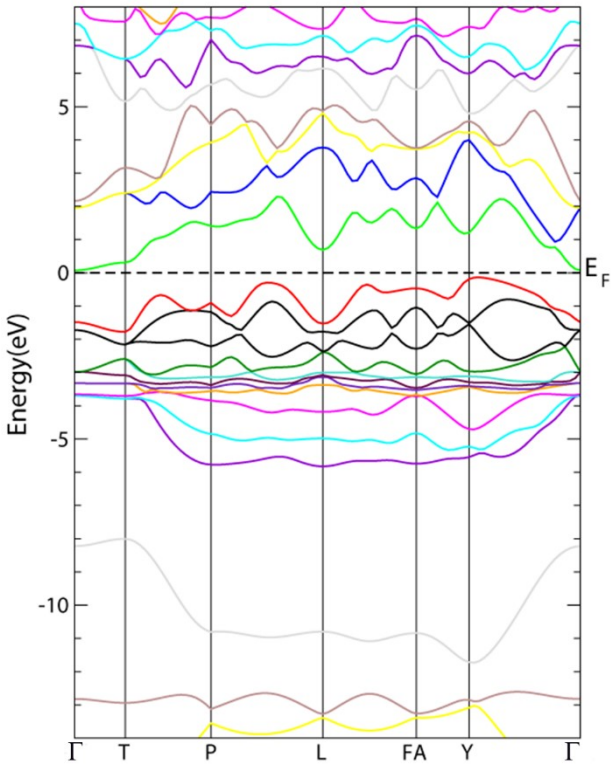

Figure.S2 Electronic band structure of β-$BiAgSe_2$

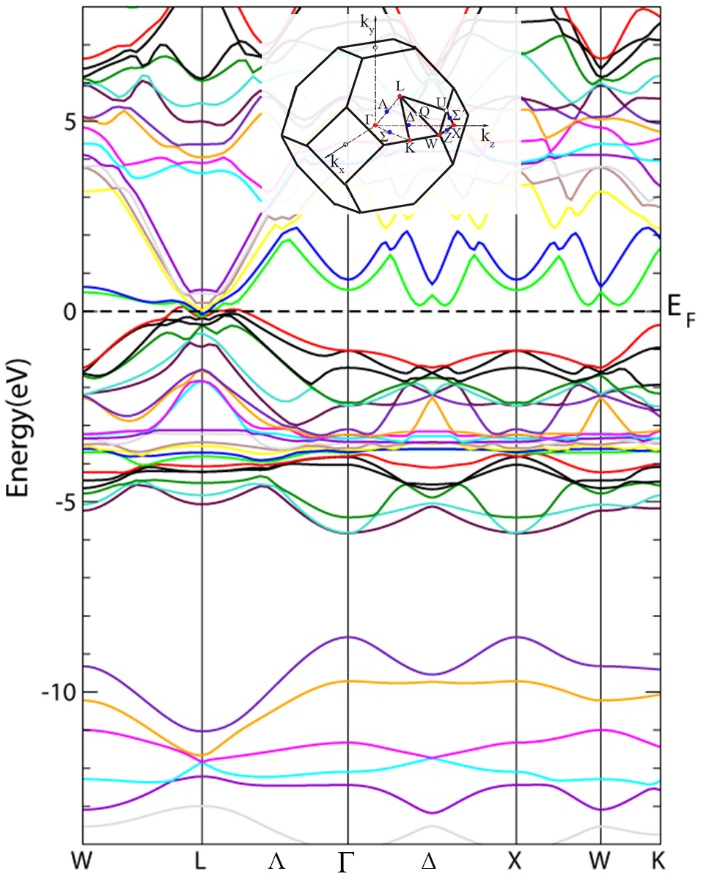

Fig.S3 Electronic Band structure of cubic BiAgSeTe; the inset figure shows the first Brillouin zone (BZ) of BiAgSeTe with high-symmetry points (red points) for calculations.

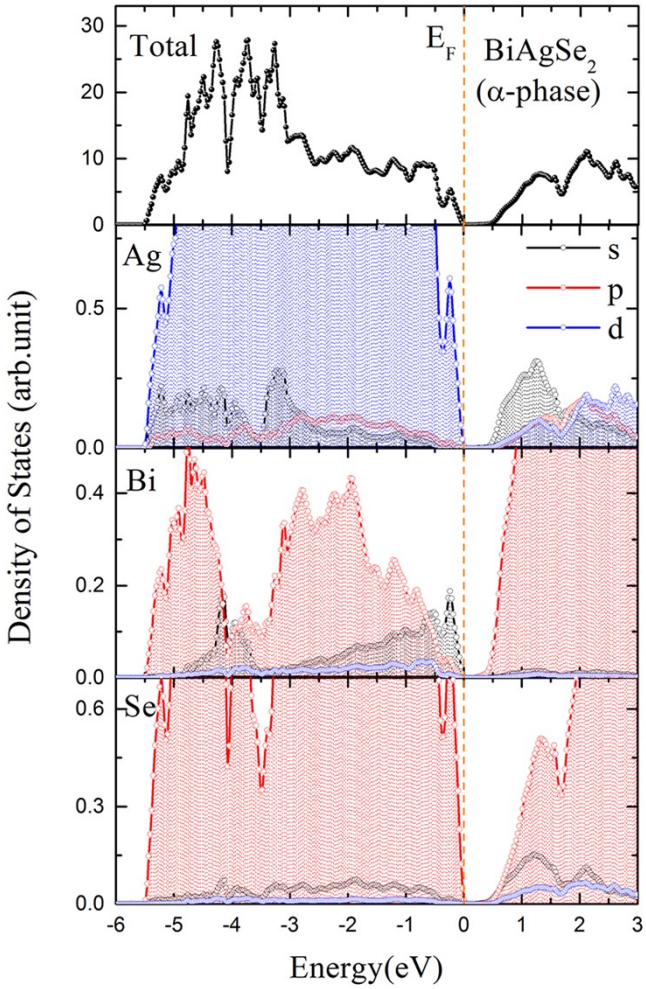

Figure.S4 Projected partial density of electronic states for α-phase $BiAgSe_2$

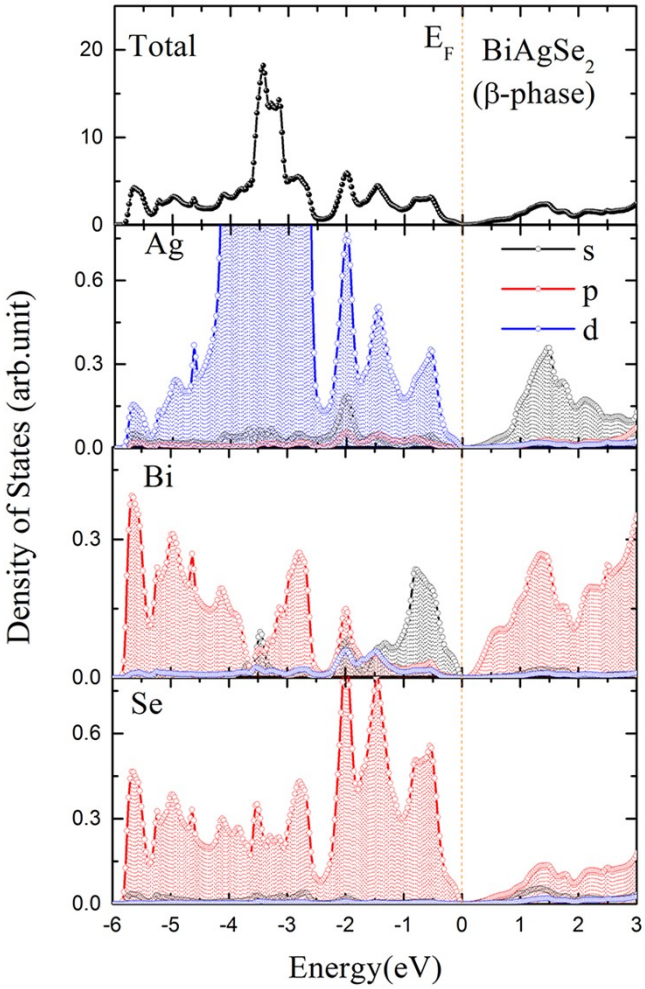

Figure.S5 Projected partial density of electronic states for β-phase $BiAgSe_2$

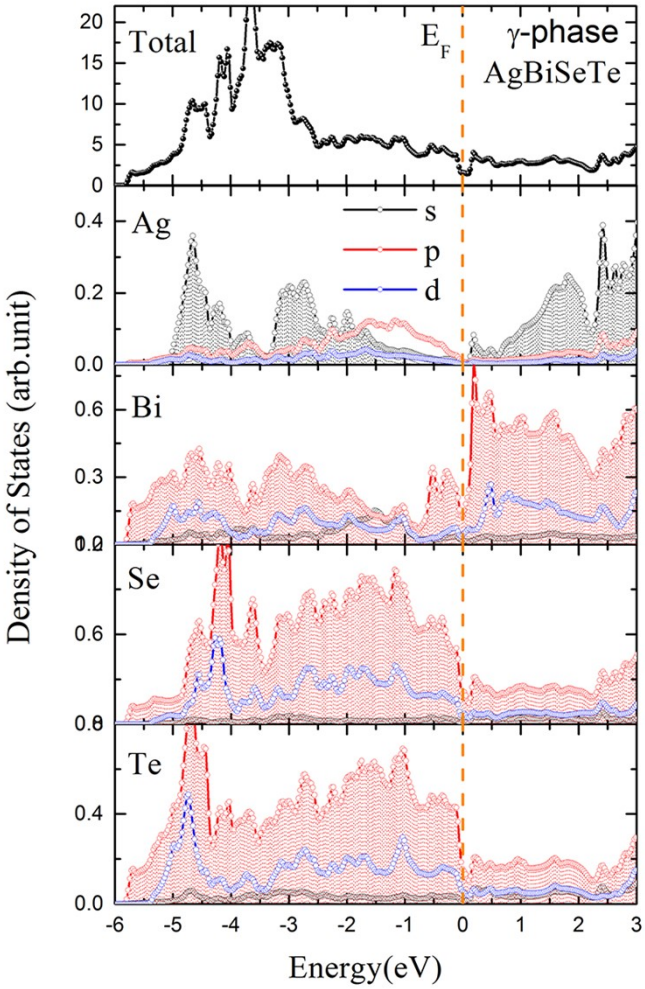

Figure.S6 Projected partial density of electronic states for γ-phase BiAgSeTe

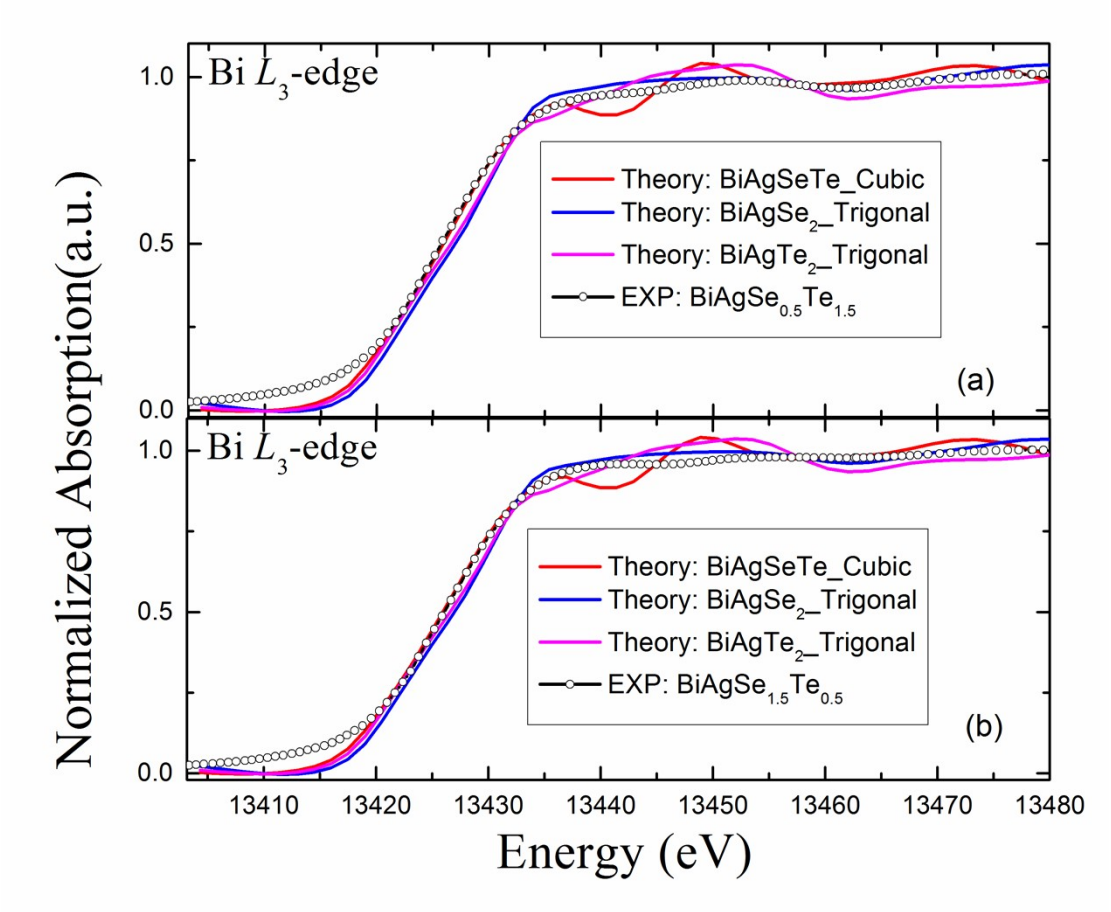

Figure.S7 Comparison of experimental and theoretical XANES spectra at Bi L_3-edge for (a) $BiAgSe_{0.5}Te_{1.5}$, (b) $BiAgSe_{1.5}Te_{0.5}$. Note that hexagonal structures were used $BiAgSe_2$ and $BiAgTe_2$ models while cubic structure was used for BiAgSeTe.

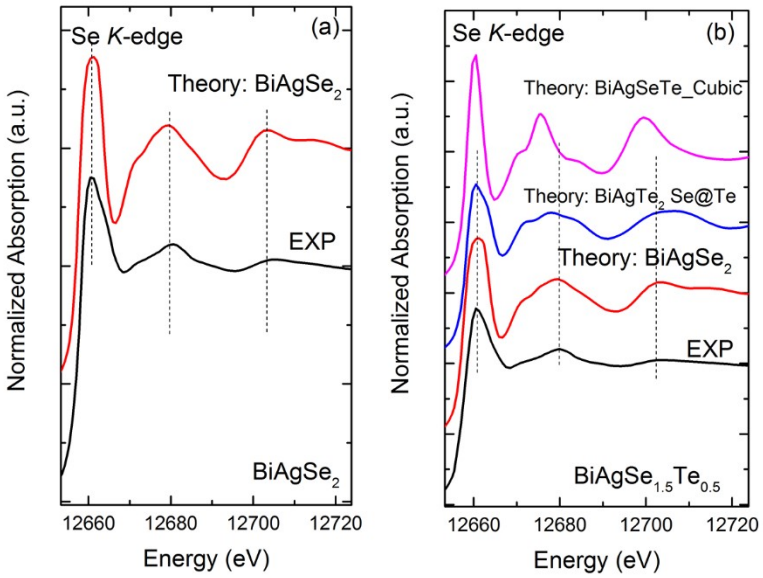

Figure.S8 Comparison of experimental and theoretical XANES spectra at Se K-edge for (a) $BiAgSe_2$ (b) $BiAgSe_{1.5}Te_{0.5}$. Note that hexagonal structures were used $BiAgSe_2$ and $BiAgTe_2$ models while cubic structure was used for BiAgSeTe.

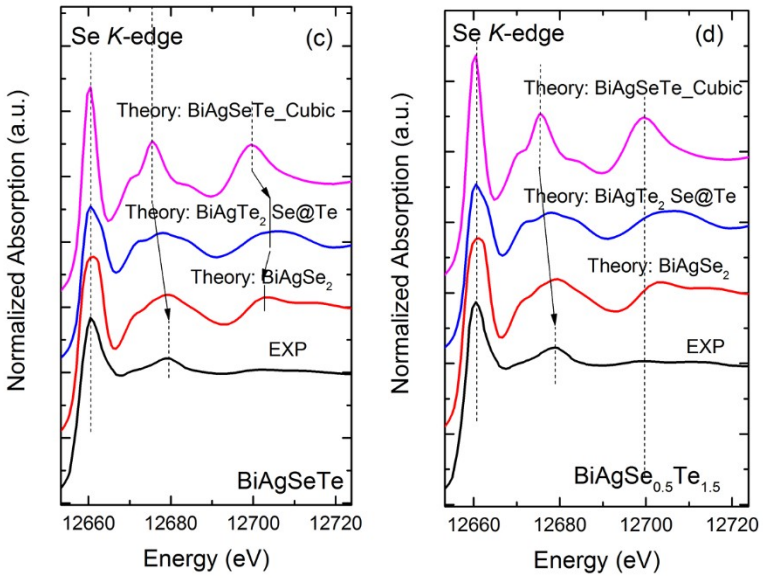

Figure.S9 Comparison of experimental and theoretical XANES spectra at Se *K*-edge for (a) BiAgSeTe (b) $BiAgSe_{0.5}Te_{1.5}$. Note that hexagonal structures were used $BiAgSe_2$ and $BiAgTe_2$ models while cubic structure was used for BiAgSeTe.

Table.S2. The electron number counts for s, p, d electrons and the differentially calculated charge transfer[1] as retrieved from the full multiple scattering theory calculations using FEFF9.0 code.

$BiAgSe_2$ Ag L_3	**S**	**P**	**D**	**CT**	**$BiAgTe_2$ Ag L_3**	**S**	**P**	**D**	**CT**
Ag	0.731	0.518	9.879	-0.128	**Ag**	0.812	0.555	9.859	-0.225
Bi	1.936	2.173	10.489	0.402	**Bi**	1.923	2.313	10.445	0.321
Se	1.977	3.868	0.293	-0.137	**Te**	1.952	3.684	0.412	-0.048
$BiAgSe_2$ Bi L_3	S	P	D	CT	**$BiAgTe_2$ Bi L_3**	S	P	D	CT
Ag	0.725	0.519	9.879	-0.123	**Ag**	0.798	0.547	9.859	-0.204
Bi	1.936	2.172	10.490	0.402	**Bi**	1.924	2.291	10.455	0.328
Se	1.976	3.859	0.305	-0.140	**Te**	1.956	3.698	10.409	-0.063
$BiAgSe_2$ Se L_3	S	P	D	CT	**$BiAgTe_2$ Te L_3**	S	P	D	CT
Ag	0.745	0.503	9.879	-0.128	**Ag**	0.823	0.539	9.860	-0.221
Bi	1.939	2.148	10.482	0.432	**Bi**	1.925	2.288	10.441	0.346
Se	1.977	3.885	0.291	-0.153	**Te**	1.951	3.704	0.407	-0.063
BiAgSeTe Ag L_3	S	P	D	CT	**BiAgSeTe Te L_3**	S	P	D	CT
Bi	1.902	2.721	10.251	0.125	**Bi**	1.968	2.128	10.366	0.536
Ag	0.590	0.546	9.835	0.029	**Ag**	0.594	0.535	9.830	0.042

Se	1.970	4.112	0.185	-0.266	**Se**	1.972	4.143	0.193	-0.309
Te	1.921	3.676	0.293	0.111	**Te**	1.929	3.778	0.298	-0.004

Table.S3 EXAFS fitting results for different structural models at the Bi L_3-edge

CN: coordination number, R: bond distance, σ^2: means square relative displacement, ΔE: energy shift; R-factor: fitting quality

Samples **k^3 weighted, k range∈(3-10) Å^{-1}** **R range∈(1.5-3)Å**	**Path**	**CN**	**R**	**σ^2 ($\times10^3$)**	**ΔE**	**R-factor**
$BiAgSe_2$-Bi_2Se_3	Bi-Se1	3.0	2.8670±0.0889	11.3±11.0	5.6±4.7	0.02
	Bi-Se2	2.7	3.0748±0.1308	13.0±5.5	5.6±4.7	
$BiAgSe_2$-β-phase	Bi-Se	1.9	2.7923±0.0336	12.0±4.6	-9.9±5.2	0.06
BiAgSeTe- Bi_2Se_3	Bi-Se1	0.8	2.8971±0.1890	31.3±7.2	18.6±15.1	0.31
	Bi-Se2	0.9	3.1330±0.4263	75.4±17.1	18.6±15.1	

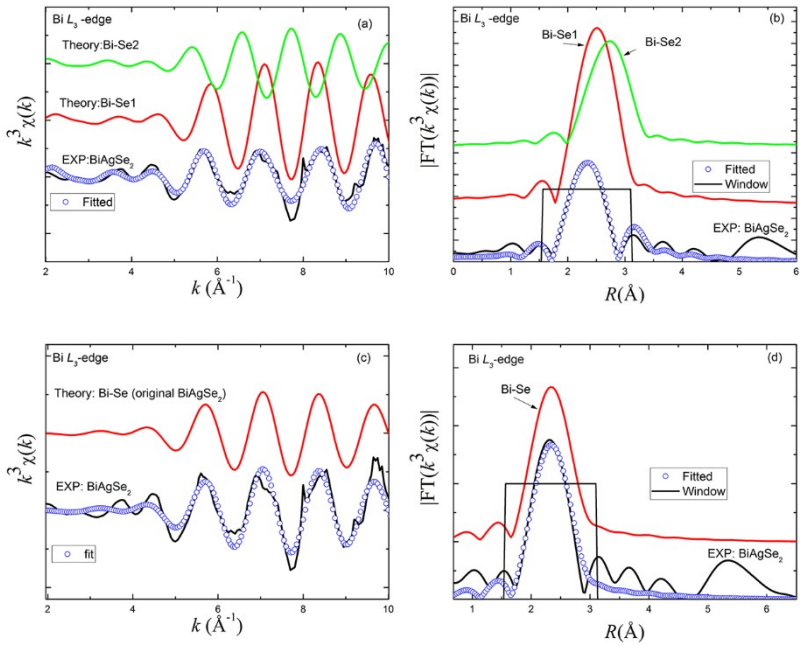

Figure.S10 Best fit of the Bi L_3-edge EXAFS of $BiAgSe_2$ in k-space (left panel) and R-space (right panel) by using (a, b) distorted model structure with two Bi-Se bond lengths and (c,d) the original hexagonal with one Bi-Se bond lengths

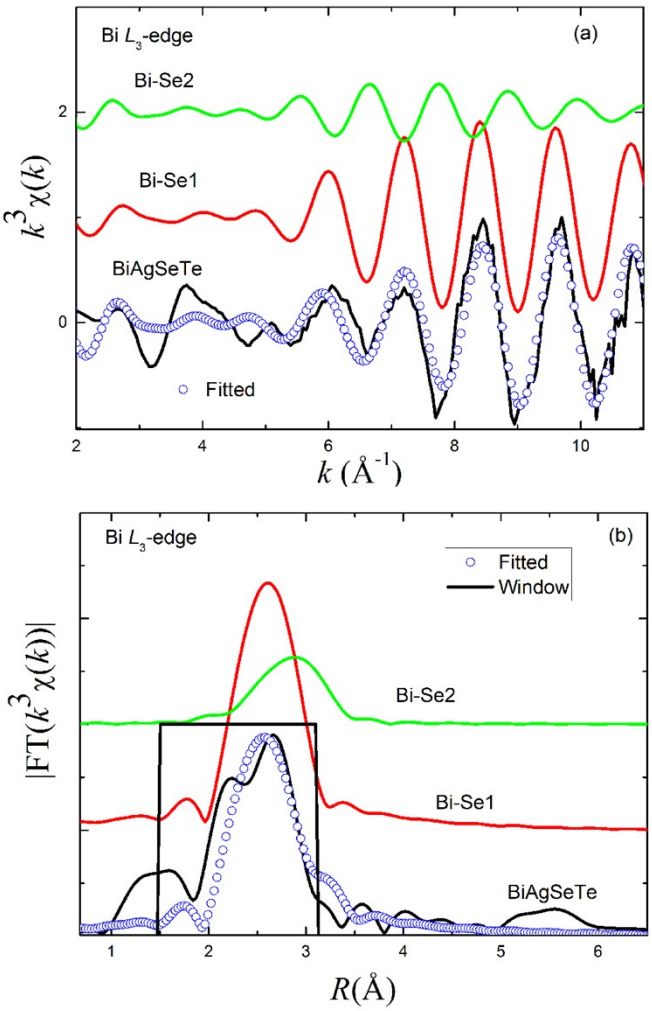

Figure.S11 Best fit of the Bi L_3-edge EXAFS of BiAgSeTe in k-space (a) and R-space (b) by using distorted model structure with two Bi-Se bond lengths

Table.S4 EXAFS fitting results for different structural models at the Se *K*-edge

$BiAgSe_2$ **k^3 weighted,** **k range∈(2.0-9.7) Å^{-1}** **R range∈(1.5-3)Å**	**Path**	**CN**	**R**	**σ^2 (×10^{-3})**	**ΔE**	**R-factor**
$BiAgSe_2$-β-phase	Se-Ag	2.7	2.7407±0.0889	26.59±11.0	1.3±1.1	0.04
	Se-Bi	2.3	2.8656±0.1308	17.0±5.5	1.3±1.1	
BiAgSeTe **k^3 weighted,** **k range∈(2.0-11) Å^{-1}** **R range∈(1-3)Å**	Path	CN	R	σ^2 (×10^{-3})	ΔE	R-factor

$BiAgSe_2$-β-phase	Se-Ag	0.3	2.6471±0.0482	12.3±6.3	2.4±0.2	0.14
	Se-Bi	2.5	2.8020±0.0817	25.6±17.8	2.4±0.2	
BiAgSeTe **k^3 weighted,** **k range∈(2.0-11) Å-1** **R range∈(1-3)Å**	Path	CN	R	σ^2 ($\times10^{-3}$)	ΔE	R-factor
$BiAgSe_2$-γ-phase	Bi-Se	0.4	2.8169±0.02	5.3±1.8	4.7±2.4	0.07
	Bi-Te	1.4	2.9926±0.07	21.7±6.1		

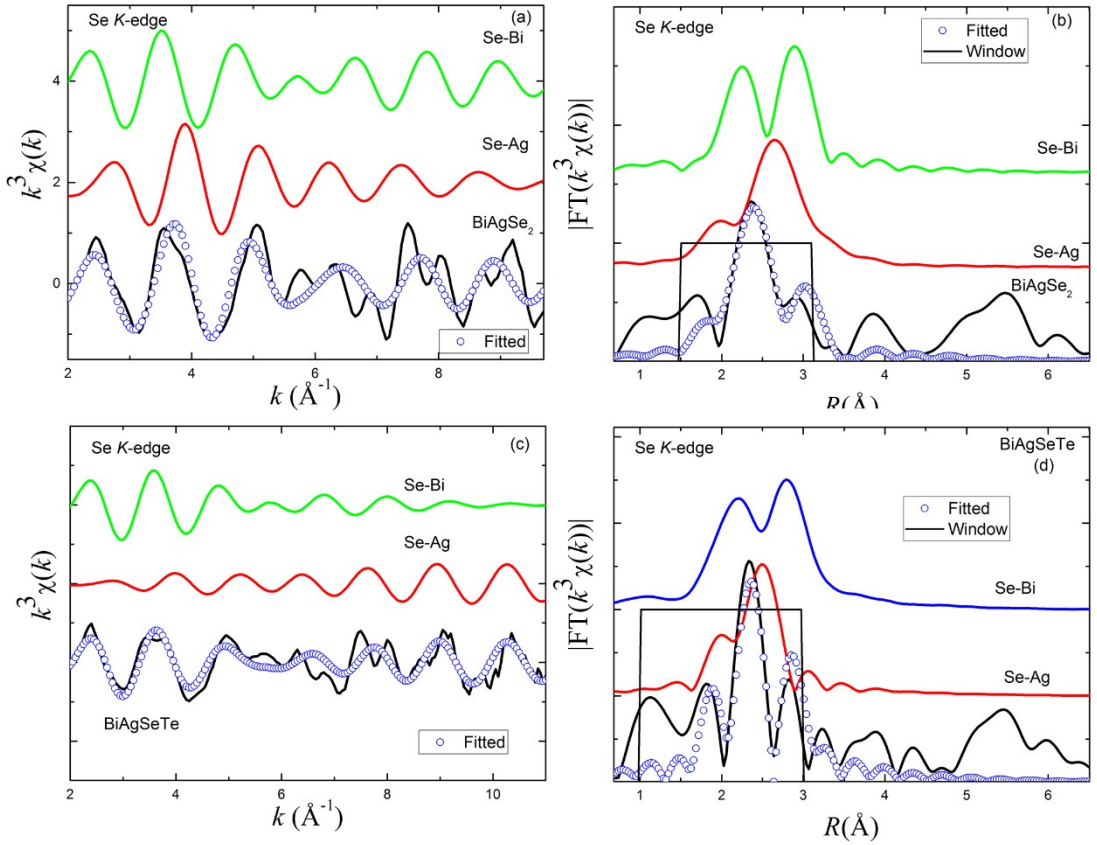

Figure.S12 Best fit of the Se *K*-edge EXAFS of $BiAgSe_2$ (a)in k-space and (b)R-space and that of BiAgSeTe (c)in k-space and (d)R-space

References

1. Ankudinov, A. L.; Ravel, B.; Rehr, J. J.; Conradson, S. D., Real-space multiple-scattering calculation and interpretation of x-ray-absorption near-edge structure. *Phys. Rev. B* **1998,** *58* (Copyright (C) 2009 The American Physical Society), 7565.